Contents lists available at ScienceDirect

Science of the Total Environment

journal homepage: www.elsevier.com/locate/scitotenv

Riparian forest response to extreme drought is influenced by climatic context and canopy structure

Ana Paula Portela [a,b,c,*], João F. Gonçalves [a,c,d], Isabelle Durance [e], Cristiana Vieira [f], João Honrado [a,b,c]

[a] CIBIO, Centro de Investigação em Biodiversidade e Recursos Genéticos, InBIO Laboratório Associado, Campus de Vairão, Universidade do Porto, 4485-661 Vairão, Portugal
[b] Departamento de Biologia, Faculdade de Ciências, Universidade do Porto, 4099-002 Porto, Portugal
[c] BIOPOLIS Program in Genomics, Biodiversity and Land Planning, CIBIO, Campus de Vairão, 4485-661 Vairão, Portugal
[d] proMetheus—Research Unit in Materials, Energy and Environment for Sustainability, Instituto Politécnico de Viana do Castelo (IPVC), Avenida do Atlântico, No. 644, 4900-348 Viana do Castelo, Portugal
[e] Water Research Institute and School of Biosciences, Cardiff University, The Sir Martin Evans Building, Museum Avenue, Cardiff CF10 3AX, United Kingdom
[f] Museu de História Natural e da Ciência da Universidade do Porto (MHNC-UP/UPorto/PRISC), Praça Gomes Teixeira, 4099-002 Porto, Portugal.

HIGHLIGHTS

- We examine the responses and resilience of riparian forests to an extreme drought.
- We found a trade-off between drought resistance and recovery.
- We found contrasting drought responses in Atlantic and Mediterranean regions.
- Overall riparian forests did not fully recover from drought after 3 years.
- Canopy structure and climatic context were the most relevant drivers of resilience.

GRAPHICAL ABSTRACT

Graphical abstract of the article showing the main findings: partial recovery of spectral indices of vegetation status 3 years following extreme drought and contrasting resistance and recovery strategies across the study area climate gradient.
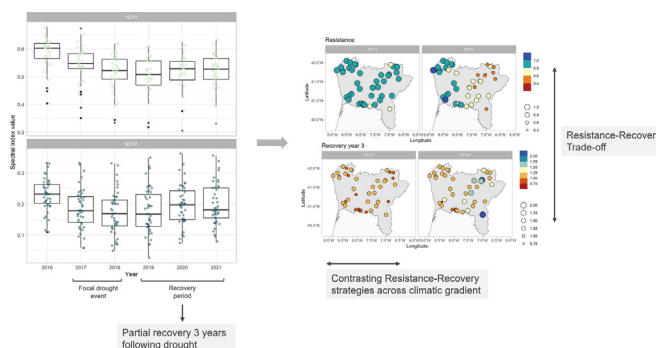
ARTICLE INFO

ABSTRACT

Droughts significantly impact forest ecosystems, reducing forest health and productivity, compromising ecosystem functioning, and nature-based solutions for climate change. The response and resilience of riparian forests to drought are poorly understood despite their key role in the functioning of aquatic and terrestrial ecosystems. Here we investigate riparian forest drought responses and resilience to an extreme drought event at a regional scale. We also examine how drought event characteristics, average climate conditions, topography, soil, vegetation structure, and functional diversity shape the resilience of riparian forests to drought. We used a time series of the Normalized Difference Vegetation Index (NDVI) and Normalized Difference Water Index (NDWI) to calculate the resistance to and recovery after an extreme drought (2017–2018) in 49 sites across an Atlantic-Mediterranean climate gradient in North Portugal. We used generalized additive models and multi-model inference to understand which factors best explained drought responses. We found a trade-off between drought resistance and recovery (maximum $r = -0.5$) and contrasting strategies across the climatic gradient of the study area. Riparian forests in the Atlantic regions showed comparatively higher resistance, while Mediterranean forests recovered more. Canopy structure and climate context were the most relevant

* Corresponding author at: CIBIO, Centro de Investigação em Biodiversidade e Recursos Genéticos, InBIO Laboratório Associado, Campus de Vairão, Universidade do Porto, 4485-661 Vairão, Portugal.
E-mail addresses: apportela@fc.up.pt (A.P. Portela), joao.goncalves@cibio.up.pt (J.F. Gonçalves), durance@cardiff.ac.uk (I. Durance), cvieira@mhnc.up.pt (C. Vieira), jhonrado@fc.up.pt (J. Honrado).

predictors of resistance and recovery. However, median NDVI and NDWI had not returned to pre-drought levels (Rc$_{NDWI}$ mean = 1.21, Rc$_{NDVI}$ mean = 1.01) three years after the event. Our study shows that riparian forests have contrasting drought response strategies and may be susceptible to extended legacy effects associated with extreme and/or recurring droughts, similarly to upland forests. This work highlights the drought vulnerability of riparian ecosystems and emphasises the need for further studies on long-term resilience to droughts.

1. Introduction

Droughts are expected to become more frequent and more severe due to climate change, which poses significant threats to human societies and ecosystems (Crausbay et al., 2017; Tramblay et al., 2020). In terrestrial ecosystems, drought reduces forest productivity and carbon sink functions, and may lead to tree mortality and possibly ecosystem transitions from forest to shrubland (Allen et al., 2015; Hammond et al., 2022). The impacts on ecosystems may propagate to human societies through declines in ecosystem services (Crausbay et al., 2017). For instance, decreases in forests' carbon sink compromise their role as nature-based solutions for climate change mitigation (Anderegg et al., 2015; Anderegg et al., 2020a).

Forest responses to drought are complex and shaped by several environmental and biological factors that determine drought resilience, the impacts on tree growth, mortality, forest communities, and ecosystem processes (Brodribb et al., 2020). Individual or species-level drought responses are driven by structural and physiological adaptations, mainly by xylem vulnerability to cavitation, but also by plant allometry, leaf area, leaf phenology, stomatal behaviour, rooting depth, and rooting strategy (Brodribb et al., 2020; Grossiord, 2020; McGregor et al., 2021). Drought responses can be more complex at the community level, as interactions between species may attenuate or exacerbate drought impacts. Interactions that attenuate drought impacts may result from resource partitioning (e.g., differential water use, shading), facilitation (e.g., hydraulic redistribution, nocturnal water release) and selection effects (dominance of drought-adapted species) (Grossiord, 2020). Forests with higher hydraulic trait diversity are less sensitive to changes in soil water and vapour-pressure deficit than forests with lower trait diversity (Anderegg et al., 2018). However, higher species diversity may also have negative or insignificant effects on drought stress (Grossiord et al., 2013; Grossiord et al., 2014). Furthermore, positive interactions may weaken or turn into negative ones under different abiotic and biotic conditions (Jucker et al., 2014; Grossiord, 2020). Landscape-level variations in topography and edaphic conditions can also modulate drought effects. A recent study showed that topography strongly shaped heatwave resilience of tree populations in Mediterranean areas (Carnicer et al., 2021). Topography has also been shown to mitigate the effects of drought on forests in valley-bottom positions (Hawthorne and Miniat, 2018).

Following a drought episode, tree damage and mortality legacies often last months or years (Schwalm et al., 2017; Brodribb et al., 2020). A global study showed that drought legacy effects are pervasive in forests and can last three to four years (Anderegg et al., 2015). In another study, post-drought temperature and precipitation conditions were strongly associated with the duration of drought recovery (Schwalm et al., 2017).

Most studies on forest's drought vulnerability focus on upland forests, typically in well-drained and deep water table sites (Fan et al., 2019; Costa et al., 2023). However, forest climate risks at regional to landscape levels remain uncertain since the drought responses of forests in topographically favourable positions, such as riparian forests, remain poorly studied (Fan et al., 2019; Costa et al., 2023).

Riparian ecosystems are relatively protected from climatic drought impacts due to their favourable geomorphic setting, which enables them to access water from precipitation, surface flow and shallow groundwater (Singer et al., 2014; Mayes et al., 2020). Nevertheless, prolonged and severe droughts can significantly affect surface water resources (Gouveia et al., 2017). Anthropogenic alterations of streamflow and groundwater abstraction to meet human demand can further lead to water stress (Palmer et al., 2008; Mac Nally et al., 2011).

Drought-related growth decline and crown dieback have been documented in riparian trees (Singer et al., 2013; Stella et al., 2013; Valor et al., 2020; Kibler et al., 2021). Increases in summer drought also caused declines in riparian plant biomass, seedling survival, and species richness (Garssen et al., 2014). Riparian vegetation productivity was shown to be positively associated with annual and seasonal precipitation (Pace et al., 2021) and negatively affected by distance to groundwater (Rohde et al., 2021) and maximum temperatures (Fu and Burgher, 2015).

The vulnerability of riparian forests to drought may impact aquatic and terrestrial ecosystems' functioning since they are central to the energy and matter exchanges between land and water (Naiman et al., 2005). Riparian plant litter inputs constitute important carbon subsidies to the aquatic food webs (Perkins et al., 2021), which may be affected by drought in their quality, amount, or timing (Sanpera-Calbet et al., 2016). The microclimate created by riparian forest shade and transpiration can help buffer streams and rivers from the effects of increasing temperatures (Ormerod and Durance, 2012) and provide habitat and shelter for terrestrial species during heatwaves (Nimmo et al., 2016). Riparian forests sequester carbon at similar or higher levels than other forests (Dybala et al., 2019). Therefore, understanding the factors underpinning riparian forests' resilience and vulnerability to drought is relevant for fundamental science and climate change mitigation and adaptation.

However, most studies on riparian responses to drought have focused on individual species' responses (Gomes Marques et al., 2018). Only recently, a few studies have assessed wider landscape-level responses either to seasonally dry conditions or local groundwater availability (Pace et al., 2021; Rohde et al., 2021). Understanding riparian ecosystems' responses to drought conditions outside their normal climatic variability and to severe or extreme events is still missing (Slette et al., 2019). We also have a limited understanding of the overall drought response strategy and resilience, particularly the ability of riparian ecosystems to maintain functioning during drought – resistance and the ability to regain functioning following drought – recovery (Lloret et al., 2011; Lloret et al., 2022).

In this work, we aim to improve the understanding of riparian forest responses and resilience to extreme droughts at the ecosystem level and across large spatial scales by addressing the following questions: (i) what are the drought response strategies of riparian forests? (ii) which factors are more relevant to explain drought resilience?, and (iii) how do they shape riparian resilience to drought?

We hypothesise that riparian forests will show declines in functioning during an extreme drought since these events affect surface water resources. However, we expect that this decline will be relatively limited due to their access to multiple water sources and modulated by diversity effects. Therefore, we expect that: (i) riparian forest drought response will be characterized by high resistance to drought; (ii) the intensity and severity of the drought event will be the main predictors of riparian forest resilience, negatively affecting resistance and recovery, and (iii) riparian forest functional diversity will modulate the impact of droughts.

2. Methods

2.1. Study area and sites

The study area comprises the North Portugal hydrographic region, divided into two biogeographical regions – the Atlantic and Mediterranean biogeographical regions (Fig. 1) (European Environment Agency, 2016a). The climate in the Atlantic biogeographical region is characterized by a stronger oceanic influence with mild winters and cool summer
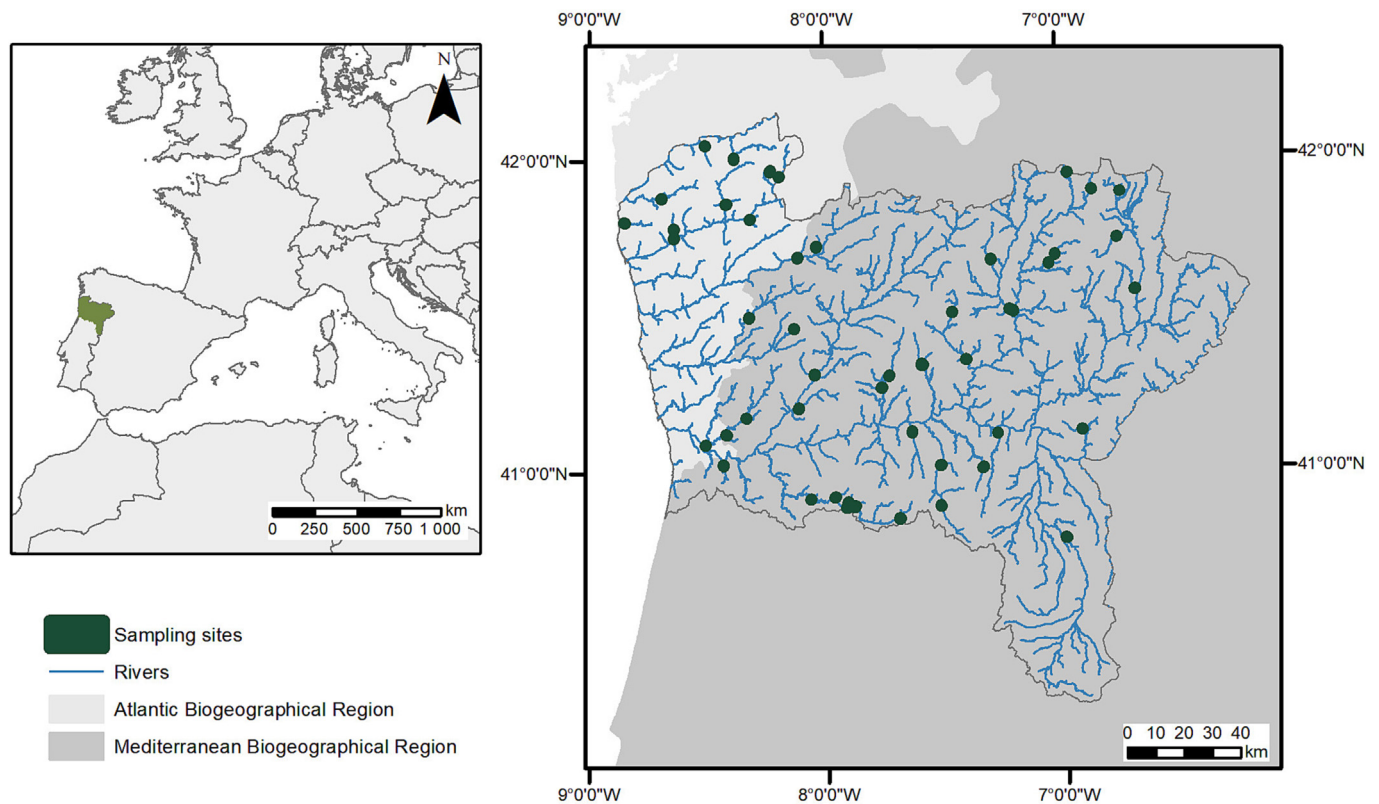
Fig. 1. Location of the study area in Europe (green area on the left) and distribution of sampling sites in the study area (right). The two European biogeographical regions encompassed by the study area are also shown (European Environment Agency, 2016a).

temperatures (European Environment Agency, 2016a). The Mediterranean biogeographical region is characterized by hot, dry summers and humid, cool winters (European Environment Agency, 2016a).

Riparian forests are dominated by alder (*Alnus lusitanica* Vít, Douda & Mandák, formerly *Alnus glutinosa* (L.) Gaertn.) in the Atlantic biogeographical region of the study area (Aguiar et al., 2013a; Amigo et al., 2017). Most riparian forests in the Mediterranean biogeographical region of the study area riparian are dominated by ash (*Fraxinus angustifolia* Vahl) (Aguiar et al., 2013a; Aguiar and Vila-Viçosa, 2017). Some alder forests persist in the Mediterranean region but are limited to large rivers with permanent flow (Aguiar and Vila-Viçosa, 2017). Willow-dominated communities (*Salix alba* L., *S. eleagnos* Scop., *S. salviifolia* Brot., *Salix × fragilis* L.) are also found in river bars or in narrow valleys with torrential winter flows in both regions (Aguiar and Vila-Viçosa, 2017; Amigo et al., 2017).

The 49 study sites are located across the study area and were surveyed in the scope of Water Framework Directive (WFD) hydromorphological monitoring (Fig. 1). We selected sites sampled in the WFD surveillance and monitoring scheme since it allowed us to access field-based data related to habitat quality, modification, and riparian structure across the study area. We used hydromorphological monitoring sites since the sampled segment (500 m) allows the inclusion of a higher number of satellite pixels than macrophyte and riparian species sampling (100 m). Hydromorphological sampling sites and assessment data were obtained from the North Regional Water Administration and correspond to fieldwork conducted during the first cycle of the River Basin Management Plans (2010–2015) (APA, 2021). Hydromorphological sampling was carried out between April and June 2010 and followed the River Habitat Survey (RHS) methodology (Environment Agency, 2003; Raven et al., 2009). The RHS methodology generally aims to assess the streams and rivers' character and habitat quality based on their physical structure (Fox et al., 1998). The field methodology systematically collects data related to substrate and flow type, bank and channel natural features and modifications, land use, presence and complexity of riparian vegetation, and stream and bank dimension along a standard 500 m length of

a river. Observations are made at ten equally spaced spot-checks at 50 m intervals, together with an overall "sweep-up" summary for the whole site. Hydromorphological quality and habitat modification are then expressed by the habitat quality assessment index (HQA) and the habitat modification score (HMS) based on the field survey information.

2.2. Photointerpretation of riparian vegetation

We used the coordinates of the first, middle and last spot-check recorded during the RHS sampling procedure to locate and delimit the sampled segments. The selection of sites for photointerpretation and delineation of the riparian forest was based on a visual inspection and measurement of forest width using Google satellite, ESRI World Imagery and Bing Virtual Earth imagery freely available in QGIS as XYZ tiles. The Copernicus "Actual riparian zone" layer (minimum mapping unit - 0.5 ha) (Weissteiner et al., 2016) and the national land cover/use dataset ("*Carta de Ocupação Solo – 2018*", minimum mapping unit - 1 ha), that includes riparian forest species in class "Other broadleaved" (DGT, 2019), helped guide the photointerpretation process when they were represented along the sampled segments. Sites where the riparian forest was mostly absent or reduced to thin single-tree lines were not included since most of the signal captured by the Sentinel-2 satellite would correspond to the surrounding land cover. For the final set of 49 sites, the riparian forests were manually digitized along the segment delimited by the spot-check coordinates using satellite and aerial imagery. To achieve better precision, we digitized riparian forests separately on the left and right banks. Patches dominated by herbaceous vegetation, bare soil, water, or other land cover types (agriculture or urban) were not included.

2.3. Drought data

We used the Standardized Precipitation-Evapotranspiration Index (SPEI) to identify drought events and spatio-temporal differences in drought

characteristics (Vicente-Serrano et al., 2010; Beguería et al., 2014). SPEI is a standardized drought index, that allows to distinguish drought from normal climatic variability (Slette et al., 2019), and compare areas with different climates at different timescales (Vicente-Serrano et al., 2013). SPEI uses monthly time series of climatic water balance, corresponding to precipitation minus the reference evapotranspiration, which is then fitted to a log-logistic probability distribution to transform the real values into standardized units (Vicente-Serrano et al., 2010; Beguería et al., 2014). Hence it encompasses variability in precipitation and evaporative demand associated with temperature. Positive SPEI values indicate wet conditions and negative values indicate dry conditions (Vicente-Serrano et al., 2010). We calculated SPEI at a 12-month timescale, i.e., the SPEI value for a given month considers data for that month and the previous 11 months (Vicente-Serrano et al., 2010; Beguería et al., 2014). The 12-month timescale can be used as an approximation to hydrological and groundwater drought (Van Loon, 2015; González-Hidalgo et al., 2018; Vicente-Serrano et al., 2021), and has been used to evaluate drought impacts on forest resilience (Gazol et al., 2018; Pace et al., 2021).

We used the TerraClimate dataset to obtain monthly precipitation and monthly reference evapotranspiration time series for each site since it provides high spatial resolution (~4 km) monthly climate data from 1958 to 2020 (Abatzoglou et al., 2018). In this dataset, potential evapotranspiration is calculated with the Penman-Monteith equation, which accounts for solar radiation, temperature, wind speed and relative humidity (Abatzoglou et al., 2018).

We calculated monthly SPEI values for each site for a 60-year interval (1962–2021) to ensure a long baseline reference (Slette et al., 2020). We defined a drought event as a period of at least two consecutive months with SPEI < −1.28. We used this threshold since it includes severe to extreme droughts (Páscoa et al., 2017; González-Hidalgo et al., 2018; Vicente-Serrano et al., 2021). SPEI values above the threshold were included in the drought event if these gaps did not exceed two months. Each drought event was characterized by: intensity – the mean SPEI value during the drought event and the lowest values – as the 5 % quantile of SPEI values during the drought event (Pérez-Luque et al., 2020). SPEI values were calculated using the "SPEI" R package (Beguería et al., 2022) and drought event detection and characterization used code from the "'heatwaveR" package adapted to monthly time series (Schlegel and Smit, 2018).

The 2017–2018 drought event analysed in this study, hereafter focal drought, corresponds to an extreme event affecting all mainland Portugal from April 2017 to February 2018 with varying intensity in space and time. According to the official drought monitoring reports, the entire mainland territory was in severe to extreme drought in October 2017, and >10 % of the territory in severe to extreme drought for nine consecutive months (IPMA, 2018). The most significant ecological and human consequences of this drought event were the large wildfires in June and October 2017, which burned a total of 500,000 ha and caused 120 fatalities (Turco et al., 2019). In freshwater ecosystems, there are also reports of significant mortalities of endangered pearl mussel populations (Nogueira et al., 2019).

The SPEI time series was also used to identify the reference year before the event, i.e., a year without drought events, and characterize the climatic conditions following the event.

2.4. Satellite data

Remote sensing allows retrospective analysis of drought responses. It provides information on temporal changes in forest primary productivity and canopy water content across large spatial scales (Huang et al., 2019; Jiao et al., 2021). We used an annual time series of two spectral indices the Normalized Difference Vegetation Index (NDVI, Eq. (1)) and the Normalized Difference Water Index (NDWI, Eq. (2)) between 2015 and 2021 to assess vegetation responses to drought. NDVI and NDWI are indicators of vegetation status and water stress (Huang et al., 2019; Jiao et al., 2021). NDVI allows quantifying the variability in forest aboveground primary productivity, and it is correlated with leaf area index (LAI) and the fraction of absorbed photosynthetically active radiation (FAPAR) (Huang

et al., 2019; Jiao et al., 2021). NDVI is also positively correlated with tree growth drought responses estimated with dendrochronological approaches (Vicente-Serrano et al., 2013; Gazol et al., 2018). NDWI is indicative of leaf water content and was shown to be responsive to drought and to have the potential to monitor forest drought stress (Huang et al., 2019; Jiao et al., 2021).

Image data were obtained from the Copernicus Sentinel-2 L1C product (European Union/ESA/Copernicus, n.d.). The high spatial and temporal resolution of Sentinel-2 opens new possibilities for effectively monitoring riparian vegetation (Huylenbroeck et al., 2020). This type of vegetation is typically distributed in narrow patches along rivers. Therefore, lower resolution satellites, including MODIS (250 m) and Landsat (30 m) are often too coarse to capture enough signal from riparian vegetation relative to its surroundings (Huylenbroeck et al., 2020; Rohde et al., 2021). NDVI and NDWI spectral indices were calculated from Sentinel-2 data as follows:

$$NDVI = \frac{\rho_{NIR} - \rho_{Red}}{\rho_{NIR} - \rho_{Red}} \quad (1)$$

$$NDWI = \frac{\rho_{NIR} - \rho_{SWIR1}}{\rho_{NIR} - \rho_{SWIR1}} \quad (2)$$

where ρ_{Red} is the red band B4 (650–680 nm), ρ_{NIR} the reflectance in the near-infrared band B8 (785–899 nm), and ρ_{SWIR1} the shortwave infrared band B11 (1565–1655 nm).

Clouds and shadows were removed from all the original Sentinel-2 images using quality layers. NDVI and NDWI image layers were aggregated annually through the mean, considering the hydrological year (from October to September). Image bands B4 and B8 have 10 m of spatial resolution while B11 has 20 m. Resampling (through the nearest-neighbour method) was employed in band B11 to match the resolution of the B4 and B8. Given Sentinel-2's high spatial resolution, NDVI/NDWI zonal aggregation per site using the mean was performed for all pixels inside the digitized riparian forest polygons. All computations were performed in Google Earth Engine geospatial cloud-computing platform (Gorelick et al., 2017).

2.5. Ecosystem resilience to drought

We estimated drought responses using two components of short-term ecosystem resilience – resistance and recovery. Resistance (Rt) is the opposite of the reduction in performance during disturbance, i.e., lower reduction means higher resistance (Lloret et al., 2011). We estimated resistance as the difference between NDWI or NDVI during the focal drought event and a reference pre-drought period (Eqs. (3-a) and (3-b)) (Lloret et al., 2011; Gazol et al., 2018).

$$R_{t,NDVI} = \frac{NDVI_{yr=2018}}{NDVI_{yr=2016}} \quad (3\text{-}a)$$

$$R_{t,NDWI} = \frac{NDWI_{yr=2018}}{NDWI_{yr=2016}} \quad (3\text{-}b)$$

To calculate the vegetation status indicators (Eqs. (3-a), (3-b), (4-a), and (4-b)), we used the hydrological year (yr), i.e., from October of $yr - 1$ to September of each year. We established 2016 as the reference year since it was the only one preceding the focal drought event with fully available Sentinel-2 data unaffected by drought events (based on the SPEI time series). We used the last year of the drought event (2018) as the drought event year.

Recovery (Rc) is the ability to regain functioning relative to the damage experienced during a disturbance, therefore measuring the difference between performance during and after disturbance (Lloret et al., 2011). We estimated recovery as the difference between NDWI and NDVI during the

focal drought event and each of the following years (from 2019 to 2021; Eqs. (4-a) and (4-b)) (Lloret et al., 2011; Gazol et al., 2018).

$$R_{c,NDVI} = \frac{NDVI_{yr=(2019,...,2021)}}{NDVI_{yr=2018}} \tag{4-a}$$

$$R_{c,NDWI} = \frac{NDWI_{yr=(2019,...,2021)}}{NDWI_{yr=2018}} \tag{4-b}$$

We calculated recovery for each of the three years following the drought event (2019, 2020, 2021), since drought legacy effects in forests can persist for three to four years in forest ecosystems (Anderegg et al., 2015). It should be noted that some sites were affected by another drought during the first year of recovery (2019).

2.6. Drivers of ecosystem resilience to drought

We compiled a set of explanatory variables related to climatic, landscape, topographic, soil, and vegetation factors influencing forest responses to drought (Table 1). These variables were grouped into focal drought event conditions, post-drought event conditions, average climatic conditions, soil, topography, habitat quality and modification, land cover/use in the site and the surroundings, canopy structure, functional and species diversity, and dominant species traits (Table 1).

The diversity and composition of riparian forest communities were estimated based on the WFD macrophyte and riparian species sampling dataset obtained in the same period as the RHS sampling. Macrophyte and riparian species sampling were conducted on a 100 m longitudinal transect, and all the vascular plant species from the channel and the margins up to the line corresponding to the average annual flooding were recorded (INAG 2008). For most sites, RHS and macrophyte sampling transects overlapped. Seven sites were excluded from further analysis as no species sampling data were available for the same river segment. Only species presence data was used to control for differences in species abundances in RHS and macrophyte sampling transects. The species dataset was filtered to include only phanerophyte species, considering the focus on riparian vegetation and the remote-sensing indicators' limited ability to detect understory vegetation.

We calculated species richness, functional diversity using Rao's quadratic entropy (Rao) for multiple and individual traits, and functional structure using the community arithmetic mean (CAM) for each trait. We used

Table 1
Final explanatory variable selection grouped by the respective variable groups and models.

Models	Variables	Variable description	Source
Focal drought event conditions	Mean absolute intensity (focal event)	Average SPEI values during the 2017–2018 drought event for each site	SPEI time series
	5 % percentile intensity (focal event)	5 % percentile of SPEI values (lowest values) during the event for each site	
Post-drought event conditions	Hydrological year average SPEI (2019) Hydrological year average SPEI (2020) Hydrological year average SPEI (2021)	Average SPEI for each recovery year and site to depict post-drought conditions	SPEI time series
Average climatic conditions	Annual average temperature (BIO_01) Precipitation seasonality (coefficient of variation, BIO_15)	Average climatic conditions (for the 1970–2000 period) for each site	WorldClim dataset (Fick and Hijmans, 2017)
	Aridity Index	Average ratio between precipitation and reference evapotranspiration for each site (increases for humid conditions)	Global Aridity Index and Potential Evapotranspiration (ET0) Climate Database (Trabucco and Zomer, 2019)
Soil	Soil % Coarse fragments Soil % Clay	Average topsoil physical properties (0-20 cm) for each site	Topsoil physical properties for Europe dataset (Ballabio et al., 2016)
Topography	Elevation (meters)	Average elevation of each site	EU-DEM dataset (European Environment Agency, 2016b)
	Topographic Wetness Index (TWI)	Average TWI of each site, (describes the tendency to accumulate water)	Calculated from EU-DEM in SAGA-GIS (Conrad et al., 2015)
Habitat quality and modification	RHS Land Use score	Score for the presence of broadleaf woodland (or native pinewood), moorland/heath, and wetland	River Habitat Survey Field Data
	RHS Tree score	Score for the continuity of trees and the presence of coarse woody debris	
	RHS Habitat modification score	Score for the degree of artificial modification to river channel morphology	
Land cover/use (site and 100 m buffer)	% cover of other broadleaf forests % cover of artificial/urban % cover agricultural land	Percentage of cover of relevant land use/cover classes in each site and the surroundings	National land cover/use dataset 2018 ("Carta de Ocupação do Solo – 2018") (DGT, 2019)
Canopy Structure	Canopy height minimum Canopy height standard deviation Canopy height median	Canopy height distribution within each sampled patch	Global Forest Canopy Height (2019) product (Potapov et al., 2021) derived from Global Ecosystem Dynamics Investigation and Landsat
Functional and species diversity	Rao multitrait	Functional diversity calculated using multiple traits (SLA, LA, SSD, height)	Macrophyte and riparian species field data and functional trait databases
	Species richness Rao SLA Rao Height	Number of species SLA functional diversity Height functional diversity	
Dominant species traits	Leaf Area Community Arithmetic Mean (CAM) Specific Leaf Area CAM Height CAM	Mean trait values for the community	Macrophyte and riparian species field data and functional trait databases

four traits related to species drought responses and general patterns of plant form and function to calculate functional diversity and structure: plant height, specific leaf area (SLA), leaf area (LA), and stem specific density (SSD) (Chave et al., 2009; Díaz et al., 2016). Xylem vulnerability to cavitation was not included due to the low trait coverage relative to the species dataset. Trait data was obtained from functional trait databases (Kleyer et al., 2008; Chave et al., 2009; Choat et al., 2012; Aguiar et al., 2013b; Tavşanoğlu and Pausas, 2018; Kattge et al., 2020) and complemented with information from the literature and floras (Castroviejo, 1986–2012; Mediavilla and Escudero, 2003; Bejarano et al., 2012; Domínguez et al., 2012; Rodríguez-Gallego et al., 2015; de la Riva et al., 2016). Duplicate entries were removed when it was possible to identify overlap between databases. Final species traits were obtained from the mean of trait values. All the selected traits covered >60 % of the total species pool. Rao was calculated using the R function "melodic" (de Bello et al., 2016), CAM was calculated using the "FD" package (Laliberté and Legendre, 2010), and trait coverage was calculated with the "traitor" package (Majekova et al., 2016).

2.7. Statistical analyses

We calculated the correlation among the drought response components (Eqs. (3-a), (3-b), (4-a), and (4-b)) to understand riparian drought response strategies. We used Generalized additive models (GAM) with Gaussian error distribution and multi-model inference to understand which predictors better explained riparian vegetation resistance and recovery. As mentioned in the previous section, we categorised candidate explanatory variables into groups (Table 1), reflecting different contributions to explain drought response. The variable selection (Table 1) was informed by knowledge derived from the literature, correlation with the two resilience components, and controlled for collinearity among candidate explanatory variables within each group (Spearman correlation ≤ 0.7 and variance inflation factors <10). GAM models were fitted for each group of explanatory variables and each resilience component. Resistance models were fitted for all groups of explanatory variables except post-drought event conditions. Recovery models were fitted for all groups of explanatory variables; however, the variable for the post-drought event conditions model varied according to the year.

The models were then ranked according to the Akaike Information Criterion with a correction for finite sample size (AICc). The best model was the one with the lowest AICc. A ΔAICc lower than four was used to select the best set of candidate models. The models' explanatory capacity was also estimated by GAM's explained deviance and the adjusted R^2. To further assess the relationship between drought indicators and each predictor, we obtained GAM response plots from the "tidymv" package (Coretta, 2022).

Statistical analysis was conducted in the R environment using the packages "Hmisc" (Harrell, 2018) and "caret" (Kuhn, 2008) for correlation analysis, "mgcv" (Wood, 2011) for GAM model construction, and "MuMIn"(Barton, 2020) for multi-model inference.

3. Results

3.1. Spatiotemporal patterns of drought resistance and recovery

We found that median NDVI and NDWI across sites declined during the years of the focal drought event (2017–2018) (Fig. 2). The first year of recovery (2019) showed similar median NDWI and even lower median NDVI than during the drought event. The second and third years of recovery showed increases in median NDVI and NDWI. However, these did not reach the median values observed for the reference year (2016).

Resistance values confirmed the decline in NDVI and NDWI throughout the study area (Rt_{NDWI} mean = 0.73, Rt_{NDVI} mean = 0.88) (Fig. 3). However, Atlantic sites, mainly located in the western part of the study area, showed generally higher resistance, hence maintaining NDWI and NDVI levels closer to the reference year (Fig. 3). In contrast, Mediterranean sites, mainly located in the inland and eastern part of the study area, showed lower resistance, reaching values for NDWI as low as 0.4, i.e., corresponding to just 40 % of the reference year (Fig. 3).

The recovery values show that most sites maintained similar or even lower NDVI and NDWI levels in the first year of recovery compared to the last year of drought (Rc_{NDWI} mean = 1.02, Rc_{NDVI} mean = 0.98, Fig. 3). NDVI and NDWI showed slight improvements in the second (Rc_{NDWI} mean = 1.20, Rc_{NDVI} mean = 1.01, Fig. 3) and third years of recovery (Rc_{NDWI} mean = 1.21, Rc_{NDVI} mean = 1.01, Fig. 3), particularly in the Mediterranean sites. However, in many sites, NDVI and NDWI levels in the third recovery year were slightly higher than in the last year of drought.

Resistance was significantly and negatively correlated with the second and third years of recovery for both vegetation status indicators (Table 2).

3.2. Main drivers of drought resistance and recovery

The canopy structure model best explained the resistance of riparian forests to drought, regardless of the vegetation status indicator (Table 3). In both models (NDVI and NDWI), canopy height standard deviation and canopy height minimum were significant predictors (Supplementary Material Table 1). In addition, the resistance-canopy structure models had the highest explained deviance.

The recovery of riparian forests following the drought event was best explained by different factors depending on the vegetation status indicator (Table 3). The recovery measured using NDVI was best explained by the soil, habitat quality and modification, and average climate models in the first year. In these models, soil clay percentage, land use score, precipitation seasonality and mean annual temperature were significant predictors (Supplementary Material Table 1). The second-year NDVI recovery was best explained by the soil and habitat quality/modification models, which had soil clay, coarse fragment percentages, land use score, and habitat modification score as significant predictors. The third-year recovery was best explained by a combination of drought and post-drought conditions, soil, dominant traits, topography and canopy structure. However, even the best model – i.e., "Focal drought event conditions"- had a much lower explained deviance than the other resistance and recovery models, which generally signals higher model uncertainty.

The first-year recovery measured using the NDWI indicator was best explained by the average climate model, which had precipitation seasonality and the aridity index as significant predictors. The second-year recovery was best explained by the average climate and canopy height models. The significant predictors in these models were the aridity index and canopy height standard deviation. The third-year recovery was best explained by the canopy height model, including again the canopy height standard deviation as a significant predictor. A few selected response plots show how significant predictors previously identified shape resistance and recovery (Figs. 4 and 5). The resistance of riparian forests to drought increased with canopy height standard deviation (Figs. 4 and 5). The first-year recovery still displayed a positive but weaker relationship with canopy height standard deviation, while the second and third years of recovery show a negative relationship (Figs. 4 and 5). Corroborating these trends, drought resistance increased, and recovery in the second and third years decreased, with the community arithmetic mean and functional divergence for height (Supplementary Material Figs. 2 and 3).

A similar inversion in the effect signal happened for the relationship between NDWI and aridity, with resistance decreasing with aridity and the second- and third-year recovery increasing with aridity (Fig. 4). The first and second years of NDVI recovery increased with the soil clay percentage and decreased with the land use score (Fig. 5).

4. Discussion

Riparian forest responses and resilience to drought events remain poorly studied despite their importance for terrestrial and aquatic ecosystems and their relevance for understanding landscape-level responses to drought (Rohde et al., 2021). Here we explored the drought response strategies of riparian forests to extreme drought and the factors underpinning forest resilience using high-resolution satellite indicators of vegetation status.
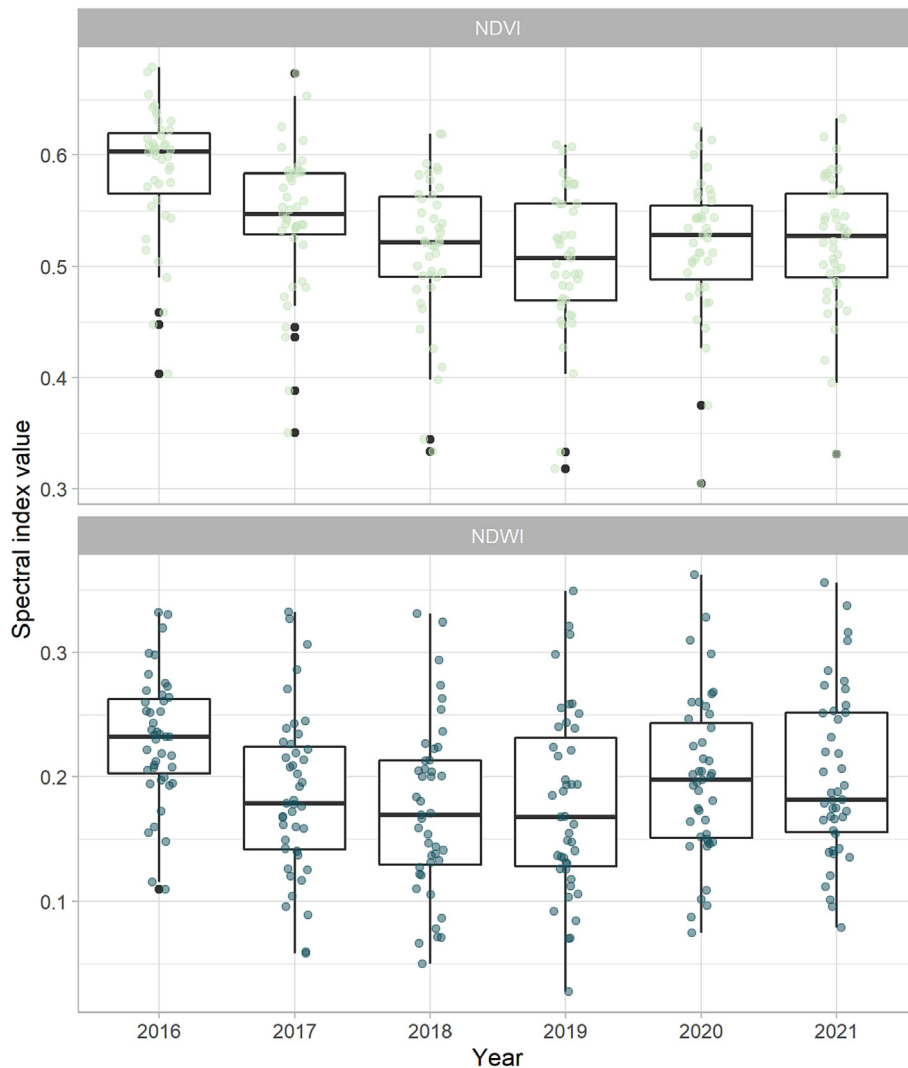
Fig. 2. NDVI and NDWI spectral indices values for study sites from 2016 to 2021. The year 2016 corresponds to the reference year, 2017–2018 correspond to the years of the focal drought event, and 2019, 2020, and 2021 correspond respectively to the first, second and third recovery years.

Our results showed that riparian forests have different drought response strategies across a regional climatic gradient and that their drought response is not only based on high resistance. Drought response strategies were influenced by climatic settings and contrasted widely between Atlantic sites, which showed high resistance and low recovery, and Mediterranean sites, which showed low resistance and high recovery. We also found that the intensity or severity of the drought event were not the main drivers of drought responses, but instead, that canopy structure and average climate conditions were the most relevant drivers of drought resistance and recovery. Soil, habitat quality and modification, and species traits also explained drought responses, but with moderate model support.

4.1. Riparian forests drought response strategies

We found a trade-off between drought resistance and recovery, suggesting two different drought response strategies across the study region. This trade-off is shown by the negative correlation between resistance and recovery (Table 2) and by the opposing trends observed for canopy structure and aridity (Figs. 4 and 5). These trends suggest that the trade-off relates to different adaptations and drought-response mechanisms under different climates (Gazol et al., 2017). Under arid conditions, riparian forests appear to control water losses more strongly and/or sooner, leading to sharper declines in photosynthetic activity and canopy water content that is compensated by new leaves and/or xylem repair after drought (Gazol et al., 2017; Volaire,

2018). Similar trade-offs have been reported for upland forests across biomes in Spain (Gazol et al., 2018) and across the northern hemisphere (Gazol et al., 2017). The different drought response strategies may also be related to differences in dominant species and acclimation of species with larger distributions to aridity and drought (Gazol et al., 2018). In a study of co-occurring rear edge populations of alder and narrow-leaved ash the two species displayed contrasting drought response strategies (Gomes Marques et al., 2018). The alder, typically dominant in the Atlantic region, showed higher resistance, while the more Mediterranean ash showed higher resilience (Gomes Marques et al., 2018). Intra-specific response variability and acclimation of alder in Mediterranean rivers is also possible, as alder has shown constant growth resilience despite increased drought frequency (Gomes Marques et al., 2018). Drought strategies were also shown to differ across populations of maritime pine (*Pinus pinaster* Aiton), with trees from wetter sites showing higher resistance and trees from drier sites showing higher recovery (Sánchez-Salguero et al., 2018). Nevertheless, further studies are required to understand the underlying mechanisms of this trade-off as it remains poorly understood (Gazol et al., 2018).

4.2. Drivers of riparian forest response and how they shape resilience

The fact that drought intensity and severity were not the best predictors of resistance or recovery was unexpected, considering the existing literature reporting a coupling between riparian vegetation productivity and
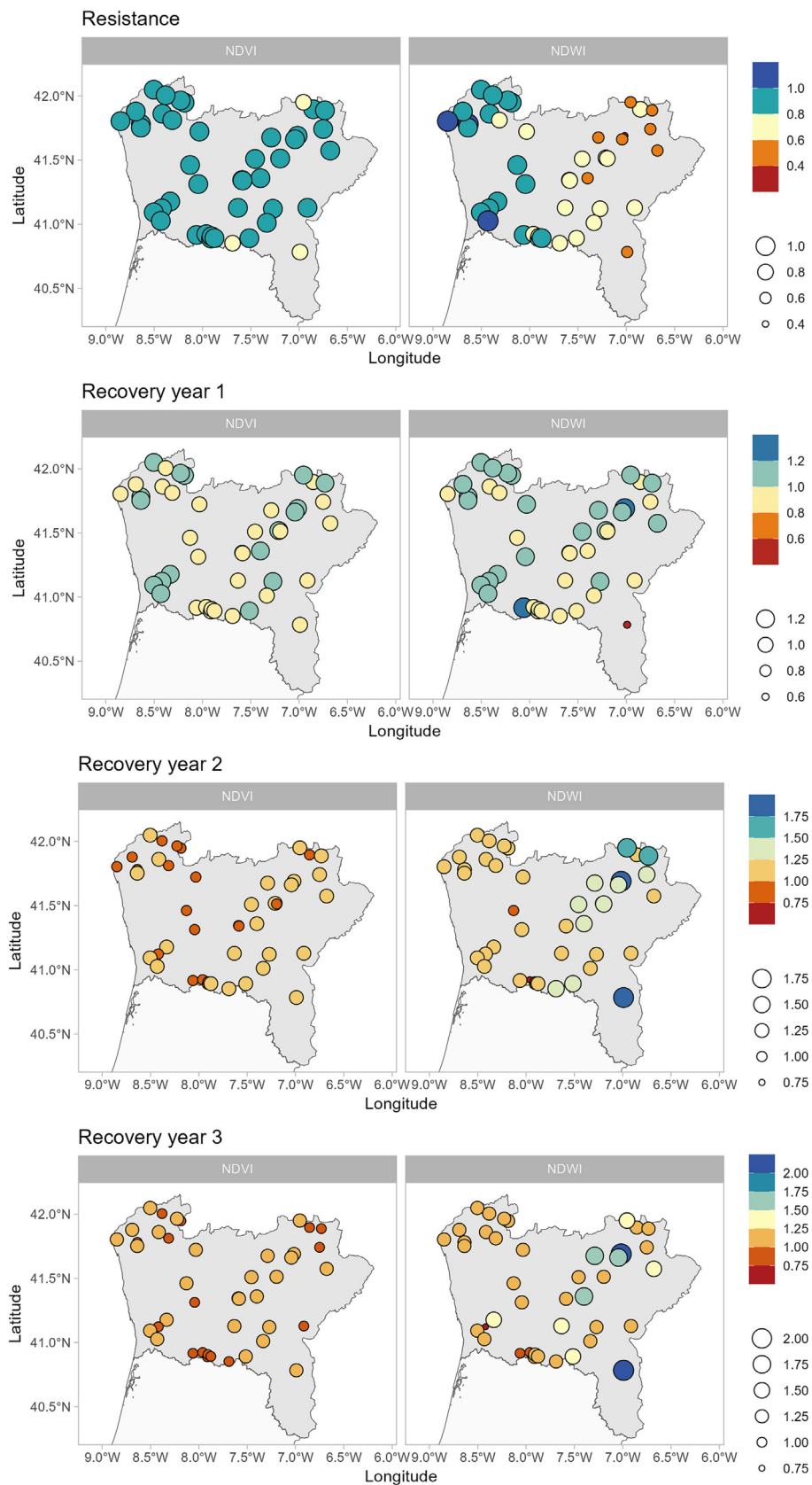
Fig. 3. Geographical patterns of resistance and recovery from the focal drought event based on NDVI and NDWI spectral indices. Higher resistance values indicate smaller declines in the spectral indices during the drought event. Higher recovery values indicate a larger increase in the spectral indices relative to the drought event.

Table 2
Pearson correlation between the drought response components. Significant correlations are shown in bold and significance levels are signalled with asterisks (*** $p < 0.001$, ** $p < 0.01$, * $p < 0.05$). NDWI – Normalized Difference Water Index and NDVI – Normalized Difference Vegetation Index.

		NDWI				NDVI			
		Resistance	Recovery year 1	Recovery year 2	Recovery year 3	Resistance	Recovery year 1	Recovery year 2	Recovery year 3
NDWI	Resistance								
	Recovery year 1	0.12							
	Recovery year 2	−**0.72*****	0.1						
	Recovery year 3	−**0.66*****	−0.01	**0.74****					
NDVI	Resistance	**0.73****	0.24	−**0.47****	−**0.45****				
	Recovery year 1	0.07	**0.56*****	0.29	0.13	0.15			
	Recovery year 2	−**0.50*****	0.01	**0.64*****	**0.63*****	−**0.31***	**0.55*****		
	Recovery year 3	−**0.37***	−0.18	**0.36***	**0.62*****	−**0.45****	0.12	**0.57*****	

annual and seasonal precipitation (Garssen et al., 2014; Pace et al., 2021). However, other studies analysing drought responses in large numbers of tree species across several biomes also reported that drought resilience, its components, and the magnitude of legacy effects were not strongly linked to drought intensity (DeSoto et al., 2020).

The most important factor explaining riparian vegetation resistance, regardless of the vegetation status indicator, was related to vertical canopy structure, particularly the canopy height standard deviation and minimum. Communities with higher canopy standard deviation, hence with more diverse vertical structures and higher minimum canopy height, showed higher resistance (Figs. 4 and 5). This trend was corroborated by the height functional structure and divergence response plots (Supplementary Material Figs. 2 and 3). This suggests that higher resistance may be related to stand structure, namely tree size and age, as well as phanerophyte species heights. This result was unexpected as taller trees are generally considered more susceptible to drought due to the higher likelihood of xylem embolism associated with the greater water transport distance and higher water column tension (Olson et al., 2018; Stovall et al., 2019; McGregor et al., 2021). However, taller trees with deeper root systems can access deeper soil moisture or groundwater during drought. Taller, older trees with deeper root systems have been linked with lower sensitivity to drought in tropical forests (Giardina et al., 2018; Schwartz et al., 2019).

Nevertheless, considering that the strongest positive effect is related to differences in tree height, this also suggests a beneficial effect of structural and functional diversity on community-level drought resistance. This beneficial effect may be related to resource partitioning or facilitation (Grossiord, 2020). There is some research suggesting that both mechanisms may occur in riparian forests, namely differential use of vadose and phreatic zone water by riparian tree species (Singer et al., 2013) and facilitation of understory herbaceous riparian function by hydraulic lift (passive transport of moisture from deeper wet soil layers to shallower dry layers by root systems) during drier years (Barron-Gafford et al., 2021).

The positive effect of structural diversity and the resistance-recovery trade-off appears to lead to a lower recovery of canopy water content. Canopy water content recovery was lower under more humid climate conditions and more diverse canopy structures. These trends suggest a compound effect of the contrasting drought response strategies and the likely depletion of soil water resources during drought in structurally diverse communities, leading to lower recovery rates.

Conversely, the recovery of canopy photosynthetic activity is mainly explained by soil and habitat conditions. NDVI recovery in the first and second year was higher in sites with higher topsoil clay content and lower land use scores. Both effects were unexpected considering the literature and suggest the need for further studies. First, the positive effect of clay content on the recovery of photosynthetic activity may be limited to the relatively low clay percentages of soils in the study area (Ballabio et al., 2016). In other studies, including broader gradients of clay content (exceeding 40 %), it negatively affected forest drought response and led to stronger legacy effects (Kannenberg et al., 2019). Second, the negative effect of the land use score may be conflated with response strategies and canopy structure. The sites with higher land use scores (i.e., ≥6) were located in the Atlantic region or transition areas and displayed extensive broadleaf woodland cover. Furthermore, we have fewer sites with high land use scores. These results suggest further studies are needed across larger gradients and within each biogeographical region to understand better the effects of soil texture and habitat quality on drought recovery.

Table 3
Model selection table for all response metrics, showing only the top-supported models with ΔAICc <4. DevExpl – Explained deviance, VIF – Variance Inflation Factor, n – number of modeling terms in the model, AICc – Akaike Information Criterion with finite size correction, ΔAICc – delta AICc between the "best" and each other candidate model, w_i – Akaike weights for each model.

Response indicator	Model	DevExpl	VIF	n	AICc	ΔAICc	w_i
NDVI							
Resistance	Canopy structure	0.428	6.124	3	−127.748	0.000	0.892
Recovery 1st year	Soil	0.276	1.057	2	−152.662	0.000	0.551
	Habitat quality and modification	0.308	1.086	3	−151.207	1.455	0.266
	Average climate conditions	0.276	1.356	3	−148.768	3.893	0.079
Recovery 2nd year	Soil	0.281	1.057	2	−132.223	0.000	0.711
	Habitat quality and modification	0.306	1.119	3	−129.325	2.898	0.167
Recovery 3rd year	Focal drought event conditions	0.140	1.009	2	−129.746	0.000	0.373
	Post-drought event conditions	0.029	–	1	−128.715	1.032	0.223
	Soil	0.069	1.606	2	−126.712	3.034	0.082
	Dominant species traits	0.088	1.365	3	−126.378	3.368	0.069
	Topography	0.020	1.036	2	−125.883	3.864	0.054
	Canopy structure	0.089	3.947	3	−125.832	3.914	0.053
			NDWI				
Resistance	Canopy structure	0.699	6.320	3	−67.065	0.000	0.999
Recovery 1st year	Average climate conditions	0.383	1.519	3	−61.001	0.000	0.951
Recovery 2nd year	Average climate conditions	0.414	1.945	3	−19.523	0.000	0.629
	Canopy structure	0.402	4.233	3	−17.919	1.605	0.282
Recovery 3rd year	Canopy structure	0.364	4.235	3	−1.949	0.000	0.875

One of the main limitations of this work is related to the currently restricted timeframe of the Sentinel-2 archive, whose launch dates to mid-2015. This fact prevents us from establishing a more extended reference period to compare with the drought event or avoid subsequent droughts during recovery. Nevertheless, similar approaches based on

fixed intervals before and after the drought events have also been used in the literature to study drought effects (Gazol et al., 2018), and our results appear consistent with previous studies for other forests. Another limitation of this work is related to species, functional traits and structural data. The lack of species abundances and xylem hydraulic vulnerability data may
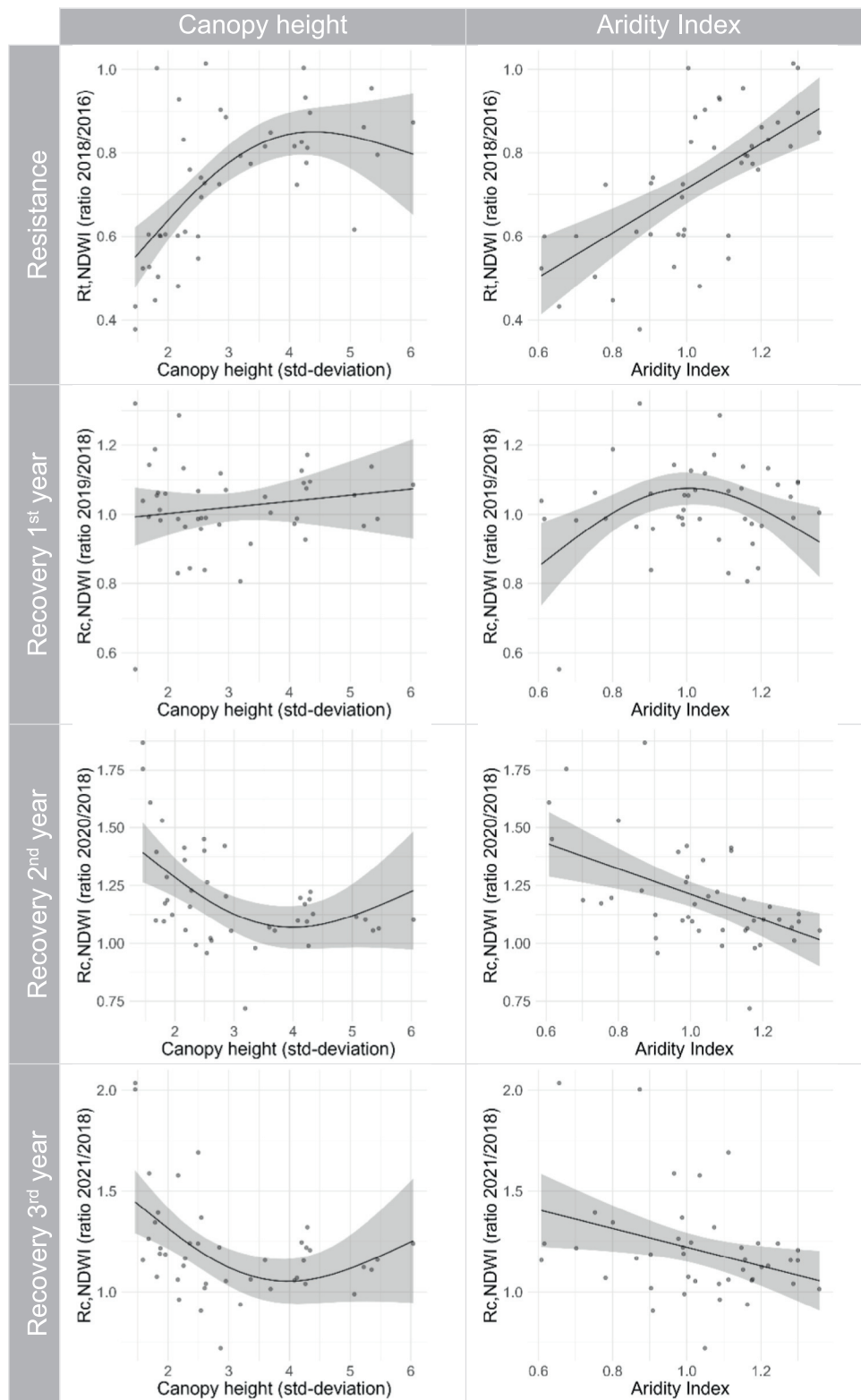
Fig. 4. Selected response plots for NDWI drought response indicators based on the models with highest support and respective significant predictors. The response plot selection reflects the most relevant models identified in the model selection table and the variable from those models that showed higher explanatory capacity. Note that aridity index values decrease with more arid conditions.
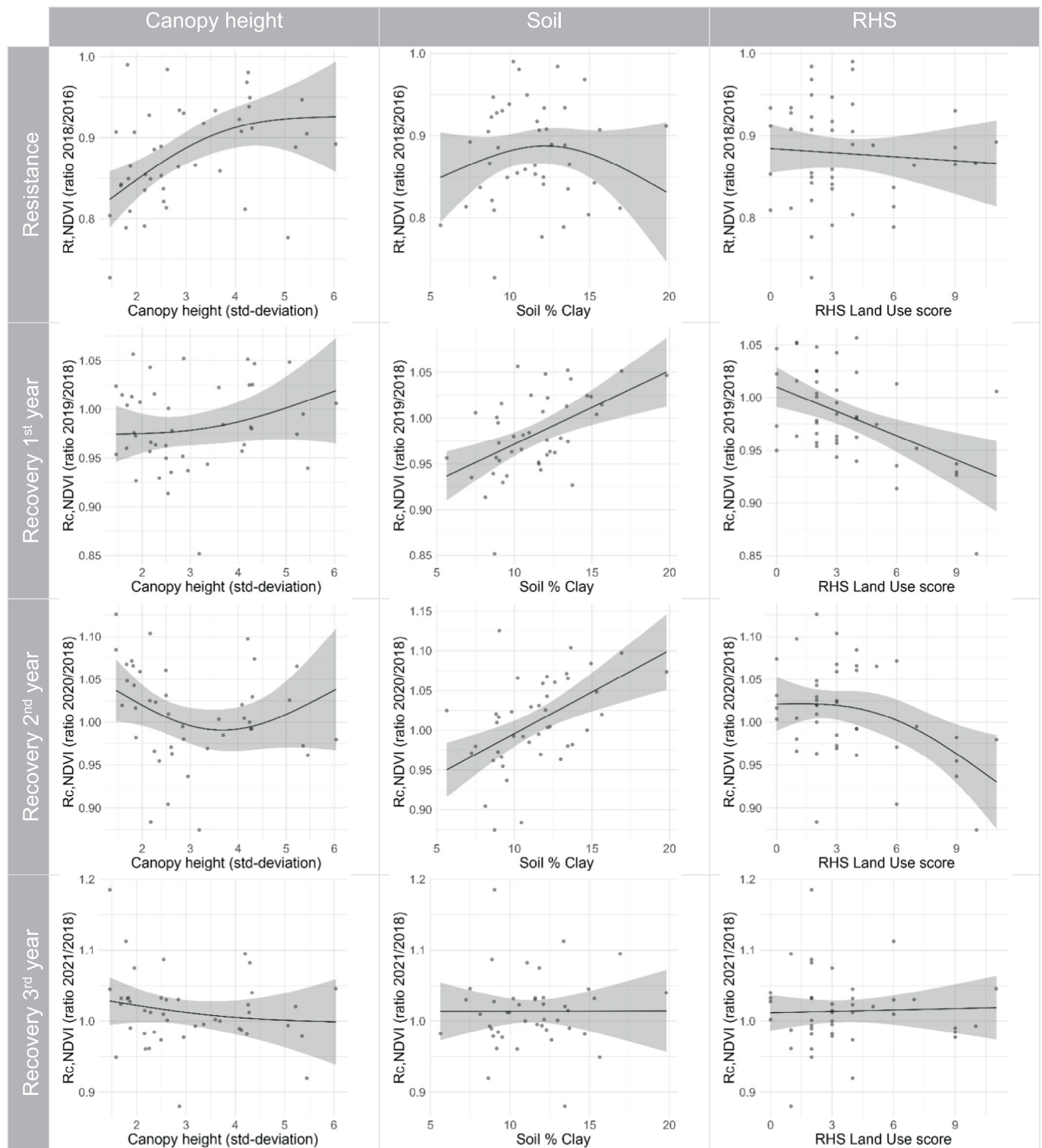
Fig. 5. Selected response plots for NDVI drought response indicators based on the models with the highest support and respective significant predictors. The response plot selection reflects the most relevant models identified in the model selection table and the variable from those models that showed higher explanatory capacity.

lead to an underestimation of the effect of functional diversity on drought resilience. Additional forest structure data (e.g., age distribution) could also improve our understanding of the canopy structure effect. However, this requires additional work to tackle gaps in functional trait data, improve the match between field and satellite data and collect further species and structural data.

4.3. Future research and management implications

Overall, our results also show that three years after the drought event, riparian forests did not return to levels of photosynthetic activity or canopy water content similar to the reference year. This result may be related to the legacy effects of the focal drought event or the fact that some sites were

affected by a subsequent drought in the first year of recovery. The currently limited timeframe of Sentinel-2 satellite data does not allow us to disentangle these two effects. Further studies are required, first to understand if drought legacy effects are as widespread in riparian forests as in other upland forests and how long they last (Anderegg et al., 2015; Kannenberg et al., 2020). Second, to understand if drought frequencies that exceed recovery times significantly impact recovery and whether this translates into long-term declines in ecosystem functioning or forest mortality that may lead to lower resilience (Anderegg et al., 2020b). Additional follow-up studies are also needed to understand the effects of drought timing on riparian forests' seasonality and phenology, since the intra-annual seasonal dynamics of drought response and legacies are still poorly understood (Pace et al., 2021).

Our results suggest that maintaining and promoting riparian communities with higher structural diversity, including taller and older trees, can enhance drought resistance, particularly in Atlantic areas. However, the trade-off between resistance and recovery observed across biogeographical regions raises doubts about whether promoting resistance is beneficial for long-term resilience and whether this is appropriate for Mediterranean regions. Recent studies suggest that promoting resistance may be beneficial in some cases. Drought resistance in angiosperms has been linked to lower long-term mortality risk in individual trees (DeSoto et al., 2020). Slower recovery rates have also been hypothesised to represent acclimation to drought, as growth reductions and wood anatomical adjustments can improve resistance to recurrent droughts and, thus, long-term survival (Gessler et al., 2020). Moreover, a recent meta-analysis did not find support for a generalized negative effect of competition on drought resilience despite common recommendations for forest thinning (Castagneri et al., 2021). To improve management strategies, further studies are required to understand the contributions of different resilience components to long-term resilience and the effects of structural and functional diversity on resilience under similar climatic settings.

5. Conclusion

Droughts significantly impact ecosystems, raising several concerns about their ability to sustain ecosystem services, particularly those mitigating climate change effects. Here we present novel insights on the resilience of riparian forests to drought at the landscape level using two complementary satellite-based indicators of vegetation status. We show that riparian forests across a regional gradient present a trade-off between resistance and recovery similar to upland forests and that drought responses are shaped by climatic gradients and vertical canopy structure. Our results also suggest that riparian forests may be susceptible to drought legacies and/or repeated drought events. There is a clear need to further investigate the long-term resilience of these forests to droughts, whether drought legacies are widespread, and if recurring events have significant negative long-term effects. Understanding riparian resilience to drought and its underlying drivers enables us to improve our fundamental understanding of forest responses to drought as well as the vulnerability of riparian forests to climate change. It also provides essential insights for adaptive management aiming to improve drought resistance and the risks posed for nature-based solutions to climate change.

CRediT authorship contribution statement

Ana Paula Portela: Conceptualization, Data curation, Methodology, Formal analysis, Writing – original draft, Writing – review & editing. **João Gonçalves:** Conceptualization, Data curation, Methodology, Formal analysis, Writing – original draft, Writing – review & editing. **Isabelle Durance:** Conceptualization, Methodology, Writing – review & editing. **Cristiana Vieira:** Methodology, Writing – review & editing. **João Honrado:** Methodology, Writing – review & editing.

Data availability

Data will be made available on request.

Declaration of competing interest

The authors have no conflict of interest to declare.

Appendix A. Supplementary data

Supplementary data to this article can be found online at https://doi.org/10.1016/j.scitotenv.2023.163128.

References

Abatzoglou, J.T., Dobrowski, S.Z., Parks, S.A., Hegewisch, K.C., 2018. TerraClimate, a high-resolution global dataset of monthly climate and climatic water balance from 1958–2015. Sci. Data 5, 170191.

Aguiar, C., Vila-Viçosa, C., 2017. Trás-Os-Montes and Beira Alta. In: Loidi, J. (Ed.)The Vegetation of the Iberian PeninsulaVolume 1. Springer International Publishing, Cham, pp. 367–394.

Aguiar, F.C., Cerdeira, J.O., Martins, M.J., Ferreira, M.T., Pillar, V., 2013a. Riparian forests of Southwest Europe: are functional trait and species composition assemblages constrained by environment? J. Veg. Sci. 24, 628–638.

Aguiar, F.C., Fabião, A.M., Bejarano, M.D., Merritt, D.M., Nilsson, C., Martins, M.J., 2013. FLOWBASE–a riparian plant traitbase. Centro de Estudos Florestais, Instituto Superior de Agronomia, Universidade de Lisboa, Lisbon.

Allen, C.D., Breshears, D.D., McDowell, N.G., 2015. On underestimation of global vulnerability to tree mortality and forest die-off from hotter drought in the Anthropocene. Ecosphere 6.

Amigo, J., Rodríguez-Guitián, M.A., Honrado, J.P., Alves, P., 2017. The lowlands and midlands of northwestern Atlantic Iberia. In: Loidi, J. (Ed.), The Vegetation of the Iberian Peninsula. 1. Springer, Cham, pp. 191–250.

Anderegg, W.R.L., Schwalm, C., Biondi, F., Camarero, J.J., Koch, G., Litvak, M., et al., 2015. Pervasive drought legacies in forest ecosystems and their implications for carbon cycle models. Science 349, 528–532.

Anderegg, W.R.L., Konings, A.G., Trugman, A.T., Yu, K., Bowling, D.R., Gabbitas, R., et al., 2018. Hydraulic diversity of forests regulates ecosystem resilience during drought. Nature 561, 538–541.

Anderegg, W.R.L., Trugman, A.T., Badgley, G., Anderson, C.M., Bartuska, A., Ciais, P., et al., 2020. Climate-driven risks to the climate mitigation potential of forests. Science 368, eaaz7005.

Anderegg, W.R.L., Trugman, A.T., Badgley, G., Konings, A.G., Shaw, J., 2020.. Divergent forest sensitivity to repeated extreme droughts. Nat. Clim. Chang. 10, 1091–1095.

APA, 2021. IP. 1.° Ciclo de planeamento (2010-2015). https://apambiente.pt/agua/1o-ciclo-de-planeamento-2010-2015.

Ballabio, C., Panagos, P., Monatanarella, L., 2016. Mapping topsoil physical properties at European scale using the LUCAS database. Geoderma 261, 110–123.

Barron-Gafford, G.A., Knowles, J.F., Sanchez-Cañete, E.P., Minor, R.L., Lee, E., Sutter, L., et al., 2021. Hydraulic redistribution buffers climate variability and regulates grass-tree interactions in a semiarid riparian savanna. Ecohydrology 14, e2271.

Barton, K., 2020. MuMIn: Multi-model Inference.

Beguería, S., Vicente-Serrano, S.M., Reig, F., Latorre, B., 2014. Standardized precipitation evapotranspiration index (SPEI) revisited: parameter fitting, evapotranspiration models, tools, datasets and drought monitoring. Int. J. Climatol. 34, 3001–3023.

Beguería, S., Vicente-Serrano, S.M., Beguería, M.S., 2022. SPEI: Calculation of the Standardised Precipitation-Evapotranspiration Index.

Bejarano, M.D., González del Tánago, M., de Jalón, D.G., Marchamalo, M., Sordo-Ward, Á., Solana-Gutiérrez, J., 2012. Responses of riparian guilds to flow alterations in a Mediterranean stream. J. Veg. Sci. 23, 443–458.

de Bello, F., Carmona, C.P., Leps, J., Szava-Kovats, R., Partel, M., 2016. Functional diversity through the mean trait dissimilarity: resolving shortcomings with existing paradigms and algorithms. Oecologia 180, 933–940.

Brodribb, T.J., Powers, J., Cochard, H., Choat, B., 2020. Hanging by a thread?Forests and drought. Science 368, 261–266.

Carnicer, J., Vives-Ingla, M., Blanquer, L., Méndez-Camps, X., Rosell, C., Sabaté, S., et al., 2021. Forest resilience to global warming is strongly modulated by local-scale topographic, microclimatic and biotic conditions. J. Ecol. 109, 3322–3339.

Castagneri, D., Vacchiano, G., Hacket-Pain, A., DeRose, R.J., Klein, T., Bottero, A., 2021. Meta-analysis reveals different competition effects on tree growth resistance and resilience to drought. Ecosystems 25, 30–43.

Castroviejo, S., 1986-2012. Flora iberica 1-8, 10-15, 17-18, 21. Real Jardín Botánico, CSIC, Madrid.

Chave, J., Coomes, D., Jansen, S., Lewis, S.L., Swenson, N.G., Zanne, A.E., 2009. Towards a worldwide wood economics spectrum. Ecol. Lett. 12, 351–366.

Choat, B., Jansen, S., Brodribb, T.J., Cochard, H., Delzon, S., Bhaskar, R., et al., 2012. Global convergence in the vulnerability of forests to drought. Nature 491, 752–755.

Conrad, O., Bechtel, B., Bock, M., Dietrich, H., Fischer, E., Gerlitz, L., et al., 2015. System for automated geoscientific analyses (SAGA) v. 2.1.4. Geosci. Model Dev. 8, 1991–2007.

Coretta, S., 2022. tidymv: Tidy Model Visualisation for Generalised Additive Models.

Costa, F.R.C., Schietti, J., Stark, S.C., Smith, M.N., 2023. The other side of tropical forest drought: do shallow water table regions of Amazonia act as large-scale hydrological refugia from drought? New Phytol. 237, 714–733.

Crausbay, S.D., Ramirez, A.R., Carter, S.L., Cross, M.S., Hall, K.R., Bathke, D.J., et al., 2017. Defining ecological drought for the twenty-first century. Bull. Am. Meteorol. Soc. 98, 2543–2550.

DeSoto, L., Cailleret, M., Sterck, F., Jansen, S., Kramer, K., Robert, E.M.R., et al., 2020. Low growth resilience to drought is related to future mortality risk in trees. Nat. Commun. 11, 545.

DGT, 2019. Carta de Uso e Ocupação do Solo - 2018.

Díaz, S., Kattge, J., Cornelissen, J.H., Wright, I.J., Lavorel, S., Dray, S., et al., 2016. The global spectrum of plant form and function. Nature 529, 167–171.

Domínguez, M.T., Aponte, C., Pérez-Ramos, I.M., García, L.V., Villar, R., Marañón, T., 2012. Relationships between leaf morphological traits, nutrient concentrations and isotopic signatures for Mediterranean woody plant species and communities. Plant Soil 357, 407–424.

Dybala, K.E., Matzek, V., Gardali, T., Seavy, N.E., 2019. Carbon sequestration in riparian forests: a global synthesis and meta-analysis. Glob. Chang. Biol. 25, 57–67.

Environment Agency, 2003. River Habitat Survey in Britain and Ireland: Field Survey Guidance Manual: 2003 Version 1: Forest Research. Environment Agency, UK.

European Environment Agency, 2016a. Biogeographical Regions.

European Environment Agency, 2016b. European Digital Elevation Model (EU-DEM), version 1.1.

European Union/ESA/Copernicus, .. Harmonized Sentinel-2 MSI: MultiSpectral Instrument, Level-1C https://developers.google.com/earth-engine/datasets/catalog/COPERNICUS_S2_HARMONIZED#description.

Fan, Y., Clark, M., Lawrence, D.M., Swenson, S., Band, L.E., Brantley, S.L., et al., 2019. Hillslope hydrology in global change research and earth system modeling. Water Resour. Res. 55, 1737–1772.

Fick, S.E., Hijmans, R.J., 2017. WorldClim 2: new 1-km spatial resolution climate surfaces for global land areas. Int. J. Climatol. 37, 4302–4315.

Fox, P.J.A., Naura, M., Scarlett, P., 1998. An account of the derivation and testing of a standard field method, river habitat survey. Aquat. Conserv. Mar. Freshwat. Ecosyst. 8, 455–475.

Fu, B., Burgher, I., 2015. Riparian vegetation NDVI dynamics and its relationship with climate, surface water and groundwater. J. Arid Environ. 113, 59–68.

Garssen, A.G., Verhoeven, J.T., Soons, M.B., 2014. Effects of climate-induced increases in summer drought on riparian plant species: a meta-analysis. Freshw. Biol. 59, 1052–1063.

Gazol, A., Camarero, J.J., Anderegg, W.R.L., Vicente-Serrano, S.M., 2017. Impacts of droughts on the growth resilience of northern hemisphere forests. Glob. Ecol. Biogeogr. 26, 166–176.

Gazol, A., Camarero, J.J., Vicente-Serrano, S.M., Sanchez-Salguero, R., Gutierrez, E., de Luis, M., et al., 2018. Forest resilience to drought varies across biomes. Glob. Chang. Biol. 24, 2143–2158.

Gessler, A., Bottero, A., Marshall, J., Arend, M., 2020. The way back: recovery of trees from drought and its implication for acclimation. New Phytol 228, 1704–1709.

Giardina, F., Konings, A.G., Kennedy, D., Alemohammad, S.H., Oliveira, R.S., Uriarte, M., et al., 2018. Tall amazonian forests are less sensitive to precipitation variability. Nat. Geosci. 11, 405–409.

Gomes Marques, I., Campelo, F., Rivaes, R., Albuquerque, A., Ferreira, M.T., Rodríguez-González, P.M., 2018. Tree rings reveal long-term changes in growth resilience in southern European riparian forests. Dendrochronologia 52, 167–176.

González-Hidalgo, J.C., Vicente-Serrano, S.M., Peña-Angulo, D., Salinas, C., Tomas-Burguera, M., Beguería, S., 2018. High-resolution spatio-temporal analyses of drought episodes in the western Mediterranean basin (Spanish mainland, Iberian Peninsula). Acta Geophysica 66, 381–392.

Gorelick, N., Hancher, M., Dixon, M., Ilyushchenko, S., Thau, D., Moore, R., 2017. Google earth engine: planetary-scale geospatial analysis for everyone. Remote Sens. Environ. 202, 18–27.

Gouveia, C.M., Trigo, R.M., Beguería, S., Vicente-Serrano, S.M., 2017. Drought impacts on vegetation activity in the Mediterranean region: an assessment using remote sensing data and multi-scale drought indicators. Glob. Planet. Chang. 151, 15–27.

Grossiord, C., 2020. Having the right neighbors: how tree species diversity modulates drought impacts on forests. New Phytol 228, 42–49.

Grossiord, C., Granier, A., Gessler, A., Jucker, T., Bonal, D., 2013. Does drought influence the relationship between biodiversity and ecosystem functioning in boreal forests? Ecosystems 17, 394–404.

Grossiord, C., Granier, A., Ratcliffe, S., Bouriaud, O., Bruelheide, H., Checko, E., et al., 2014. Tree diversity does not always improve resistance of forest ecosystems to drought. Proceedings of the National Academy of Sciences 111, 14812–14815.

Hammond, W.M., Williams, A.P., Abatzoglou, J.T., Adams, H.D., Klein, T., Lopez, R., et al., 2022. Global field observations of tree die-off reveal hotter-drought fingerprint for Earth's forests. Nat. Commun. 13, 1761.

Harrell, F.E., 2018. Hmisc: Harrell Miscellaneous.

Hawthorne, S., Miniat, C.F., 2018. Topography may mitigate drought effects on vegetation along a hillslope gradient. Ecohydrology 11, e1825.

Huang, C.-y., Anderegg, W.R.L., Asner, G.P., 2019. Remote sensing of forest die-off in the Anthropocene: from plant ecophysiology to canopy structure. Remote Sens. Environ. 231.

Huylenbroeck, L., Laslier, M., Dufour, S., Georges, B., Lejeune, P., Michez, A., 2020. Using remote sensing to characterize riparian vegetation: a review of available tools and perspectives for managers. J. Environ. Manag. 267, 110652.

IPMA, 2018. Situação de Seca Meteorológica. https://www.ipma.pt/resources.www/docs/im.publicacoes/edicoes.online/20180406/pryhFYgszRoHXedniacN/cli_20180331_2018331_sec_mm_co_pt.pdf.

Jiao, W., Wang, L., McCabe, M.F., 2021. Multi-sensor remote sensing for drought characterization: current status, opportunities and a roadmap for the future. Remote Sens. Environ. 256.

Jucker, T., Bouriaud, O., Avacaritei, D., Dănilă, I., Duduman, G., Valladares, F., et al., 2014. Competition for light and water play contrasting roles in driving diversity-productivity relationships in iberian forests. J. Ecol. 102, 1202–1213.

Kannenberg, S.A., Maxwell, J.T., Pederson, N., D'Orangeville, L., Ficklin, D.L., Phillips, R.P., 2019. Drought legacies are dependent on water table depth, wood anatomy and drought timing across the eastern US. Ecol. Lett. 22, 119–127.

Kannenberg, S.A., Schwalm, C.R., Anderegg, W.R.L., 2020. Ghosts of the past: how drought legacy effects shape forest functioning and carbon cycling. Ecol. Lett. 23, 891–901.

Kattge, J., Bonisch, G., Diaz, S., Lavorel, S., Prentice, I.C., Leadley, P., et al., 2020. TRY plant trait database - enhanced coverage and open access. Glob. Chang. Biol. 26, 119–188.

Kibler, C.L., Schmidt, E.C., Roberts, D.A., Stella, J.C., Kui, L., Lambert, A.M., et al., 2021. A brown wave of riparian woodland mortality following groundwater declines during the 2012–2019 California drought. Environ. Res. Lett. 16.

Kleyer, M., Bekker, R.M., Knevel, I.C., Bakker, J.P., Thompson, K., Sonnenschein, M., et al., 2008. The LEDA traitbase: a database of life-history traits of the northwest european flora. J. Ecol. 96, 1266–1274.

Kuhn, M., 2008. Building predictive models in R using the caret package. J. Stat. Softw. 28, 1–26.

Laliberté, E., Legendre, P., 2010. A distance-based framework for measuring functional diversity from multiple traits. Ecology 91, 299–305.

Lloret, F., Keeling, E.G., Sala, A., 2011. Components of tree resilience: effects of successive low-growth episodes in old ponderosa pine forests. Oikos 120, 1909–1920.

Lloret, F., Jaime, L.A., Margalef-Marrase, J., Perez-Navarro, M.A., Batllori, E., 2022. Short-term forest resilience after drought-induced die-off in southwestern european forests. Sci. Total Environ. 806, 150940.

Mac Nally, R., Cunningham, S.C., Baker, P.J., Horner, G.J., Thomson, J.R., 2011. Dynamics of Murray-Darling floodplain forests under multiple stressors: the past, present, and future of an Australian icon. Water Resour. Res. 47.

Majekova, M., Paal, T., Plowman, N.S., Bryndova, M., Kasari, L., Norberg, A., et al., 2016. Evaluating functional diversity: missing trait data and the importance of species abundance structure and data transformation. PLoS One 11, e0149270.

Mayes, M., Caylor, K.K., Singer, M.B., Stella, J.C., Roberts, D., Nagler, P., 2020. Climate sensitivity of water use by riparian woodlands at landscape scales. Hydrol. Process. 34, 4884–4903.

McGregor, I.R., Helcoski, R., Kunert, N., Tepley, A.J., Gonzalez-Akre, E.B., Herrmann, V., et al., 2021. Tree height and leaf drought tolerance traits shape growth responses across droughts in a temperate broadleaf forest. New Phytol. 231, 601–616.

Mediavilla, S., Escudero, A., 2003. Relative growth rate of leaf biomass and leaf nitrogen content in several mediterranean woody species. Plant Ecol. 168, 321–332.

Naiman, R.J., Décamps, H., McClain, M.E., 2005. Riparia: Ecology, conservation, and Management of Streamside Communities. Academic Press, Burlington.

Nimmo, D.G., Haslem, A., Radford, J.Q., Hall, M., Bennett, A.F., 2016. Riparian tree cover enhances the resistance and stability of woodland bird communities during an extreme climatic event. J. Appl. Ecol. 53, 449–458.

Nogueira, J.G., Lopes-Lima, M., Varandas, S., Teixeira, A., Sousa, R., 2019. Effects of an extreme drought on the endangered pearl mussel Margaritifera margaritifera: a before/after assessment. Hydrobiologia 848, 3003–3013.

Olson, M.E., Soriano, D., Rosell, J.A., Anfodillo, T., Donoghue, M.J., Edwards, E.J., et al., 2018. Plant height and hydraulic vulnerability to drought and cold. Proceedings of the National Academy of Sciences 115, 7551–7556.

Ormerod, S.J., Durance, I., 2012. Understanding and managing climate change effects on river ecosystems. River Conservation and Management. John Wiley & Sons, Ltd, pp. 107–119.

Pace, G., Gutierrez-Canovas, C., Henriques, R., Boeing, F., Cassio, F., Pascoal, C., 2021. Remote sensing depicts riparian vegetation responses to water stress in a humid Atlantic region. Sci. Total Environ. 772, 145526.

Palmer, M.A., Reidy Liermann, C.A., Nilsson, C., Flörke, M., Alcamo, J., Lake, P.S., et al., 2008. Climate change and the world's river basins: anticipating management options. Front. Ecol. Environ. 6, 81–89.

Páscoa, P., Gouveia, C.M., Russo, A., Trigo, R.M., 2017. Drought trends in the Iberian Peninsula over the last 112 years. Adv. Meteorol. 2017, 1–13.

Pérez-Luque, A.J., Gea-Izquierdo, G., Zamora, R., 2020. Land-use legacies and climate change as a double challenge to oak Forest resilience: mismatches of geographical and ecological rear edges. Ecosystems 24, 755–773.

Perkins, D.M., Durance, I., Jackson, M., Jones, J.I., Lauridsen, R.B., Layer-Dobra, K., et al., 2021. Systematic variation in food web body-size structure linked to external subsidies. Biol. Lett. 17, 20200798.

Potapov, P., Li, X., Hernandez-Serna, A., Tyukavina, A., Hansen, M.C., Kommareddy, A., et al., 2021. Mapping global forest canopy height through integration of GEDI and landsat data. Remote Sens. Environ. 253, 112165.

Raven, P.J., Holmes, N., Pádua, J., Ferreira, J., Hughes, S., Baker, L., et al., 2009. River Habitat Survey in Southern Portugal. Results from 2009. Environment Agency, Bristol.

de la Riva, E.G., Pérez-Ramos, I.M., Tosto, A., Navarro-Fernández, C.M., Olmo, M., Marañón, T., et al., 2016. Disentangling the relative importance of species occurrence, abundance and intraspecific variability in community assembly: a trait-based approach at the whole-plant level in Mediterranean forests. Oikos 125, 354–363.

Rodríguez-Gallego, C., Navarro, T., Meerts, P., 2015. A comparative study of leaf trait relationships in coastal dunes in southern Spain. Plant Ecol. Evol. 148, 57–67.

Rohde, M.M., Stella, J.C., Roberts, D.A., Singer, M.B., 2021. Groundwater dependence of riparian woodlands and the disrupting effect of anthropogenically altered streamflow. Proceedings of the National Academy of Sciences 118, e2026453118.

Sánchez-Salguero, R., Camarero, J.J., Rozas, V., Génova, M., Olano, J.M., Arzac, A., et al., 2018. Resist, recover or both? Growth plasticity in response to drought is geographically structured and linked to intraspecific variability in Pinus pinaster. J. Biogeogr. 45, 1126–1139.

Sanpera-Calbet, I., Acuña, V., Butturini, A., Marcé, R., Muñoz, I., 2016. El Niño southern oscillation and seasonal drought drive riparian input dynamics in a Mediterranean stream. Limnol. Oceanogr. 61, 214–226.

Schlegel, R.W., Smit, A.J., 2018. heatwaveR: a central algorithm for the detection of heatwaves and cold-spells. J. Open Source Softw. 3, 821.

Schwalm, C.R., Anderegg, W.R.L., Michalak, A.M., Fisher, J.B., Biondi, F., Koch, G., et al., 2017. Global patterns of drought recovery. Nature 548, 202–205.

Schwartz, N.B., Budsock, A.M., Uriarte, M., 2019. Fragmentation, forest structure, and topography modulate impacts of drought in a tropical forest landscape. Ecology 100, e02677.

Singer, M.B., Stella, J.C., Dufour, S., Piégay, H., Wilson, R.J.S., Johnstone, L., 2013. Contrasting water-uptake and growth responses to drought in co-occurring riparian tree species. Ecohydrology 6, 402–412.

Singer, M.B., Sargeant, C.I., Piegay, H., Riquier, J., Wilson, R.J., Evans, C.M., 2014. Floodplain ecohydrology: climatic, anthropogenic, and local physical controls on partitioning of water sources to riparian trees. Water Resour. Res. 50, 4490–4513.

Slette, I.J., Post, A.K., Awad, M., Even, T., Punzalan, A., Williams, S., et al., 2019. How ecologists define drought, and why we should do better. Glob. Chang. Biol. 25, 3193–3200.

Slette, I.J., Smith, M.D., Knapp, A.K., Vicente-Serrano, S.M., Camarero, J.J., Begueria, S., 2020. Standardized metrics are key for assessing drought severity. Glob. Chang. Biol. 26, e1–e3.

Stella, J.C., Riddle, J., Piégay, H., Gagnage, M., Trémélo, M.-L., 2013. Climate and local geomorphic interactions drive patterns of riparian forest decline along a Mediterranean Basin river. Geomorphology 202, 101–114.

Stovall, A.E.L., Shugart, H., Yang, X., 2019. Tree height explains mortality risk during an intense drought. Nat. Commun. 10, 4385.

Tavşanoğlu, Ç., Pausas, J.G., 2018. A functional trait database for Mediterranean Basin plants. Sci. Data 5, 180135.

Trabucco, A., Zomer, R., 2019. Global Aridity Index and Potential Evapotranspiration (ET0) Climate Database v2. figshare.

Tramblay, Y., Koutroulis, A., Samaniego, L., Vicente-Serrano, S.M., Volaire, F., Boone, A., et al., 2020. Challenges for drought assessment in the Mediterranean region under future climate scenarios. Earth Sci. Rev. 210, 103348.

Turco, M., Jerez, S., Augusto, S., Tarin-Carrasco, P., Ratola, N., Jimenez-Guerrero, P., et al., 2019. Climate drivers of the 2017 devastating fires in Portugal. Sci. Rep. 9, 13886.

Valor, T., Camprodon, J., Buscarini, S., Casals, P., 2020. Drought-induced dieback of riparian black alder as revealed by tree rings and oxygen isotopes. For. Ecol. Manag. 478, 118500.

Van Loon, A.F., 2015. Hydrological drought explained. WIREs. Water 2, 359–392.

Vicente-Serrano, S.M., Beguería, S., López-Moreno, J.I., 2010. A multiscalar drought index sensitive to global warming: the standardized precipitation evapotranspiration index. J. Clim. 23, 1696–1718.

Vicente-Serrano, S.M., Gouveia, C., Camarero, J.J., Begueria, S., Trigo, R., Lopez-Moreno, J.I., et al., 2013. Response of vegetation to drought time-scales across global land biomes. Proceedings of the National Academy of Sciences 110, 52–57.

Vicente-Serrano, S.M., Pena-Angulo, D., Murphy, C., Lopez-Moreno, J.I., Tomas-Burguera, M., Dominguez-Castro, F., et al., 2021. The complex multi-sectoral impacts of drought: evidence from a mountainous basin in the central spanish Pyrenees. Sci. Total Environ. 769, 144702.

Volaire, F., 2018. A unified framework of plant adaptive strategies to drought: crossing scales and disciplines. Glob. Chang. Biol. 24, 2929–2938.

Weissteiner, C., Ickerott, M., Ott, H., Probeck, M., Ramminger, G., Clerici, N., et al., 2016. Europe's green Arteries—A continental dataset of riparian zones. Remote Sens. 8, 925.

Wood, S.N., 2011. Fast stable restricted maximum likelihood and marginal likelihood estimation of semiparametric generalized linear models. J. R. Stat. Soc. Series B Stat. Methodol. 73, 3–36.